



**HAL**  
open science

# Theoretical Study of the Thermal Decomposition of Urea Derivatives

Jonathan Honorien, René Fournet, Pierre-Alexandre Glaude, Baptiste Sirjean

► **To cite this version:**

Jonathan Honorien, René Fournet, Pierre-Alexandre Glaude, Baptiste Sirjean. Theoretical Study of the Thermal Decomposition of Urea Derivatives. *Journal of Physical Chemistry A*, 2022, 126 (36), pp.6264-6277. 10.1021/acs.jpca.2c04291 . hal-03779258

**HAL Id: hal-03779258**

**<https://hal.science/hal-03779258v1>**

Submitted on 16 Sep 2022

**HAL** is a multi-disciplinary open access archive for the deposit and dissemination of scientific research documents, whether they are published or not. The documents may come from teaching and research institutions in France or abroad, or from public or private research centers.

L'archive ouverte pluridisciplinaire **HAL**, est destinée au dépôt et à la diffusion de documents scientifiques de niveau recherche, publiés ou non, émanant des établissements d'enseignement et de recherche français ou étrangers, des laboratoires publics ou privés.

# Theoretical Study of the Thermal Decomposition of Urea Derivatives

Jonathan Honorien<sup>1</sup>, René Fournet<sup>1</sup>, Pierre-Alexandre Glaude<sup>1</sup>, Baptiste Sirjean<sup>1,\*</sup>

<sup>1</sup> Université de Lorraine, CNRS, LRGP, F-54000 Nancy, France

Corresponding author :

Baptiste Sirjean

Laboratoire Réactions et Génie des Procédés

1 rue Grandville BP 20451 54001 Nancy Cedex,

France

Email: [baptiste.sirjean@univ-lorraine.fr](mailto:baptiste.sirjean@univ-lorraine.fr)

## **Abstract**

An extensive theoretical study of the thermal decomposition of alkyl- and phenyl-ureas, widely used in pesticides, pharmaceutical and materials industries, has been carried out using electronic structure calculations and reaction rate theories. Enthalpies of formation and bond dissociation energies (BDE) of 11 urea derivatives have been calculated using different levels of theory (CBS-QB3, CCSD(T)/CBS//M06-2X/6-311++G(3df,2pd), CBS-QM062X) according to the size of the system. Potential energy surfaces for the unimolecular decomposition pathways of these urea derivatives were also systematically computed for the first time. Several pericyclic reactions can be envisaged, as a function of the size and the nature of the N-substituents, and all these pathways were explored. Our calculations show that these compounds are solely decomposed by 4-center pericyclic reactions, yielding substituted isocyanates and amines and that initial bond fissions are not competitive. Based on the set of urea derivatives studied, a new reaction rate rule for their thermal decomposition was defined and involves the nature of the transferred H-atom (primary or secondary / alkyl or benzyl) and the nature of the N-atom acceptor (primary, secondary and tertiary). This new reaction rate rule allows to determine the products branching ratios in the thermal decomposition of a given urea derivative and its total rate of decomposition. Applications on urea derivatives used in the chemical industry are presented and illustrate the usefulness of this new rate rule that allows to predict the previously unknown thermal decomposition kinetics of a large number of these compounds.

## 1. Introduction

Nowadays, urea and its derivatives are one of the most widespread class of chemical compounds used in the industry. Historically urea was the first reported organic compound obtained from inorganic species.<sup>1</sup> The global urea production is around 200 million tons per year,<sup>2</sup> making urea a high tonnage compound. Given the ubiquitous involvement of urea and its derivatives (alkyl- and phenyl-urea) in the chemical industry, it becomes crucial to understand their reactivity during thermal degradation (accidental fires, incineration, waste recovery, etc.) and establish the main decomposition pathways to predict the degradation products and thus to better anticipate environmental or health risks.

Despite the importance of these compounds, very little is known about their decomposition kinetics under high-temperature conditions. Most of the information that can be found is thermodynamic data. The gas-phase standard enthalpies of formation of 12 alkyl-ureas (with alkyl = methyl, ethyl, isopropyl, *n*-, *s*- and *ter*-butyl ) were proposed by Kabo et al.<sup>3</sup> using combustion calorimetry, vapor formation and differential scanning calorimetry. Kozyro et al.<sup>4</sup> also proposed experimental thermodynamic data for methyl-ureas. Emel'yanenko et al.<sup>5</sup> re-explored the latter thermochemical data and supplemented it with new experimental data. They also compared theoretical calculations computed at the G3(MP2) level of theory with the experimental data and found a maximum discrepancy of 2.6 kcal/mol. More recently, Dorofeeva and Suchkova<sup>6</sup> calculated the thermochemical data of urea, alkyl-ureas and phenyl-ureas, at the G4 level of theory. They computed the enthalpies of formation of 14 ureas from a thermochemical network of 91 balanced reactions and they pointed out a possible lack of reliability of several experimental enthalpies of formation from the literature. Bodi et al.<sup>7</sup> measured the threshold for the dissociative photoionization channel of urea proposed a revise value of its enthalpy of formation using W1 and CBS-APNO calculations. Gratzfeld and Olzmann<sup>8</sup> calculated the gas-phase standard enthalpies of formation of urea pyrolysis byproducts (biuret, triuret, cyanuric acid, ammelide, ammeline and melamine) using high-level quantum chemistry methods (CCSD(F12\*)(T)/cc-pVTZ) and isodesmic reactions.

Kinetic data on the thermal decomposition of urea derivatives in the gas-phase remain scarce. Indeed, urea and most of its derivatives are solids at ambient temperature and their decomposition is heterogeneous and occurs in different states of matters. Most studies on the thermal decomposition of these compounds are based on Thermogravimetric Analysis (TGA) or Differential Scanning Calorimetry (DSC) experiments.<sup>9</sup>

Recently, there has been a significant interest in the decomposition of urea and the subsequent formation of by-products in Selective Catalytic Reduction of NO<sub>x</sub>.<sup>10,11</sup> Schaber et al.<sup>12</sup> explored the thermal degradation of urea and byproducts formation from a solid sample pyrolysis. By means of TGA and DCS experiments they provided one of the first complete reaction scheme divided into temperature-related “reaction regions”: From room temperature to 190°C urea melts and decomposes, from 190°C and 250°C biuret rises to a maximum while cyanuric acid — the main byproducts from urea thermal decomposition — increases slightly. Brack et al.<sup>13</sup> proposed a kinetic model for the thermal decomposition of urea, which was able to reproduced TGA of urea and its major by-products: biuret and cyanuric acid. The evolution of products was found in fairly good agreement with simulations. Subsequent experimental studies were performed to improve this model by revisiting kinetic data and including phase change reactions.<sup>14-16</sup>

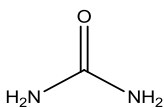
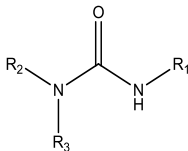
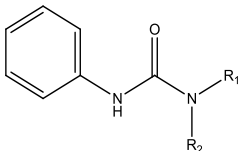
Recently, we proposed<sup>17</sup> a new pathway, based on theoretical calculations, which explains the formation of cyanuric acid, the major by-product formed in urea pyrolysis. The growth to heavier product was found to be promoted by enolic form of urea, carbamimidic acid. The mechanism proposed was able to capture the trends of the experiments of Schaber et al.<sup>12</sup>

If a few studies explored the decomposition pathways of urea using ab initio methods,<sup>18, 19</sup> to the best of our knowledge, no study investigated those of alkyl- or phenyl-urea.

This study aims to unravel the influence of the substituents of the urea derivatives on their thermal decomposition routes and kinetics using electronic structure calculations and reaction rate theories. In addition to urea, the alkyl- and phenyl-urea families were chosen to represent the most widely used compounds in the pharmaceuticals, pesticides, and organic

synthesis industries. Table 1 presents these families and examples of their applications in the chemical industry.

Table 1. Urea and its derivatives

	Urea	Alkylureas	Phenylureas
2D structure			
Use	Fertilizer, adhesives, foam insulation, animal feed...	Pesticides, intermediate in organic synthesis, pharmaceuticals...	Pesticides, pharmaceuticals, intermediate in organic synthesis ...

Based on the elementary patterns of the ureas presented in Table 1, a set of 10 representative molecules was defined in this study. In these compounds,  $R_1$ ,  $R_2$  and  $R_3$  will be H, methyl, ethyl, butyl, isopropyl and phenyl groups, in order to explore the influence of the chain length and the nature of the substituents on their decomposition routes and kinetics. Using the computed rate coefficients for all representative molecules of the training set, we propose generic rate rules for the thermal decomposition of all urea derivatives, as a function of their substituents.

## 2. Computational methods

All the electronic structure calculations were performed with Gaussian16 software.<sup>20</sup> Due to the large number of heavy atoms involved in several urea derivatives, it is necessary to use a theoretical method able to maximize the ‘accuracy/computational time’ criterion. To determine the most suitable level of calculation, we performed a benchmark on the enthalpy of formation of urea. Table 2 presents the results of our theoretical calculations using composite methods (CBS-QB3,<sup>21</sup> G4,<sup>22</sup> W1U<sup>23</sup>) and CCSD(T)/CBS//M06-2X/6-311++G(3df,2pd).<sup>24</sup> The CBS extrapolation is obtained according to the work of Martin<sup>25</sup> and involves Dunning’s cc-pVTZ and cc-pVQZ basis sets.<sup>26</sup> Enthalpies of formation at 298 K were

determined by averaging 3 isodesmic reactions, which are reported in Table S1. Literature values are also given for comparison.

Table 2. Isodesmic enthalpy of formation (in kcal mol<sup>-1</sup>) of urea (C<sub>2</sub> symmetry group) computed at different levels of calculations. Isodesmic reactions are given in Table S1. Reported uncertainties are the standard deviation of the 3 isodesmic reactions used.

Method	$\Delta_f H^\circ_{298K}$	Reference
G4	-56.2 ± 0.6	This work
CBS-QB3	-57.1 ± 0.6	This work
W1U	-56.0 ± 0.3	This work
CBS-QM06 <sup>a</sup>	-57.1 ± 0.6	This work
CCSD(T)/CBS//M06-2X/6-311++G(3df,2pd)	-56.3 ± 0.3	This work
CCSD(F12)(T)/cc-pVTZ-F12// $\omega$ B97X-D/cc-pVTZ	-55.4	Gratzfeld and Olzmann <sup>8</sup>
W1	-56.3	Bodi et al. <sup>7</sup>
G4, reaction network	-55.9	Doorofeeva and Suchkova <sup>6</sup>
Thermochemical network	-56.1 ± 0.1	ATcT <sup>27, 28</sup>
Experiments	-56.8	Emel'yanenko et al. <sup>5</sup>
Experiments	-56.3 ± 0.29	Kabo et al. <sup>3</sup>

<sup>a</sup> CBS-QB3 calculation where the geometry optimization and frequency calculations at the B3LYP/6-311G(d,p) level are replaced by M062X/6-311++G(3df,2pd).<sup>24</sup>

It can be seen in Table 2 that the gas-phase enthalpy of formation of urea ranges between -57.1 and -55.4 kcal/mol. Doorofeeva and Suchkova<sup>6</sup> recently recommended to use the value of Kabo et al.<sup>3</sup> (-56.3 kcal mol<sup>-1</sup>), based on their calculations with a thermochemical network of reactions. Among the different levels of calculations tested in this work, the CCSD(T)/CBS//M06-2X/6-311++G(3df,2pd) (noted CCSD(T)/CBS hereafter) value, computed from three isodesmic reactions, agrees with the recommended experimental value. It is also the case for the N-H Bond Dissociation Energies (BDE) in urea,<sup>29</sup> presented in Table S2.

From the benchmark, we chose to systematically perform CCSD(T)/CBS calculations to determine the potential energy surfaces (PES). When the size of the molecular system is too large to apply such calculations, and therefore too large for W1U too, we decided to use CBS-QM06 calculations. It is the case for phenyl-ureas derivatives for which energy calculations at the CCSD(T)/CBS method can no longer be applied due to prohibitive

computation time and memory requirement. Based on the results given in Table 2 and S2, we decided to use the CBS-QM06 method, where the B3LYP/6-311G(d,p) level of theory used for optimization and frequency calculations is replaced by the M06-2X/6-311++G(3df,2pd) level. Using the latter level of theory allows us to remain consistent with the CCSD(T)/CBS approach, where the same level of calculation is used for geometries and frequencies. As shown in the literature, hydrogen bonding is suspected to be an important parameter in aryl-ureas thermal decomposition experiments.<sup>30</sup> The M06-2X method is known to better describe such non-bonded interactions compared to B3LYP.<sup>24</sup> In addition, the use of a more extended basis set, with diffuse functions, will allow a better description of the molecular structures that include lone pairs, and a more accurate calculation of the vibrational frequencies and therefore of partition functions.

For all the computed extrema of the PESs, T1 diagnostics were systematically performed and their values were always found below 0.02, which ensures that a single reference method can be used to describe such molecular systems.

High-pressure rate coefficients were estimated by means of canonical transition state theory. The rate constants are weighted by a statistical factor involving external symmetry and the number of optical isomers of the reactants and the transition state. Partitions functions were calculated in the Rigid Rotor – Harmonic Oscillator (RRHO) approximation, except for low vibrational frequencies corresponding to internal rotations of alkyl and phenyl groups. For these specific vibrational modes, the hindered rotor model was applied using a modified 1D-HR approach, combined with relaxed scans obtained at the M06-2X/6-311++G(3df,2pd) level of theory.<sup>31</sup> A specific treatment was performed for urea as relaxed scans of OC-N bonds led to irregular relaxed scans, with sudden changes of curvatures. Figure 1 presents the computed torsional potential around the N-C bond in urea ( $C_2$ , *anti* conformation).



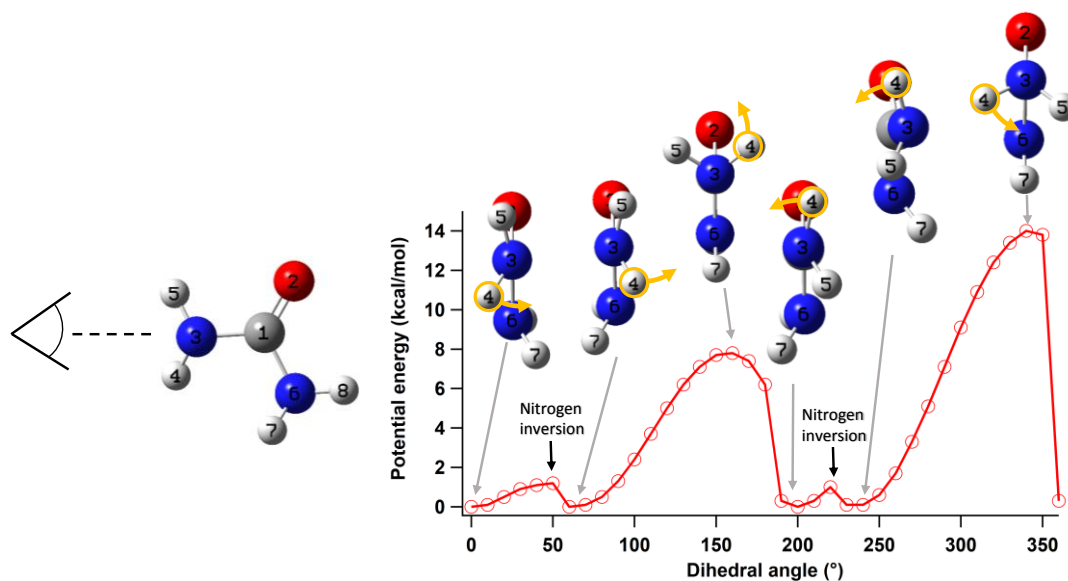
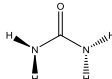
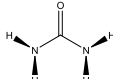


Figure 1: Relaxed scan of the dihedral angle between atoms number 6,1,2 and 4 (N-H torsion) performed at the M06-2X/6-311++G(3df,2pd). Yellow circle around hydrogen #4 and associated arrow are drawn to guide the eye.

In Figure 1, it can be seen that the computed potential features several changes in curvature due to the inversion of both nitrogen atoms of urea. The computed electronic energy barriers for the internal rotation are about 8 and 14 kcal<sup>-1</sup> mol<sup>-1</sup>. Given these relatively high-energy barriers and the shape of the torsional scan, we used a multi-structural approach for the calculation of urea partition function. Two minima can be optimized for urea: a non-symmetric C<sub>s</sub> conformation (*syn*) and a symmetric C<sub>2</sub> (*anti*) conformation.<sup>32</sup> During the course of this study, we found that the harmonic low-frequency corresponding to the torsion of a NH<sub>2</sub>-group in the C<sub>s</sub> symmetry is very sensitive to the level of calculation. Comparisons of computed torsional harmonic frequencies of NH<sub>2</sub>- groups and entropies at different levels of calculations are presented in Table 3. More comparisons are given in Table S3, where the level of theory, the basis set and the convergence criteria of geometry optimization were assessed.

Table 3. Computed total standard entropies ( $S^\circ$ ) and lowest harmonic frequencies in *syn* and *anti* urea conformations.

Optimization and frequency method	 anti, $C_2$ point group <sup>a</sup>		 syn, $C_s$ point group	
	Frequency ( $\text{cm}^{-1}$ )	$S^\circ$ (cal/mol.K)	Frequency ( $\text{cm}^{-1}$ )	$S^\circ$ (cal/mol.K)
B3LYP/6-31+G(d,p)	358.6	66.8	25.4	72.7
M062X/6-311++g(3df,2pd)	370.8	66.6	23.2	72.6
CCSD(T)/cc-pVTZ	399.4	66.3	401.1	65.9
EXP	445.1 <sup>33,b</sup>			

<sup>a</sup>In the RRHO approximation, the *anti* conformer has a chirality of 2<sup>b</sup> gas phase, low-temperature experiments in Ar-matrix

For the *anti* conformation of urea, DFT and CCSD(T) results are consistent for the computed lowest vibrational frequency (around  $400 \text{ cm}^{-1}$ ). This leads to values of entropies ranging between  $66.3$  and  $66.8 \text{ cal mol}^{-1} \text{ K}^{-1}$ . However, for the *syn* conformation, the calculated lowest vibrational frequencies with DFT methods are below  $100 \text{ cm}^{-1}$ , which yields entropies around  $73 \text{ cal mol}^{-1} \text{ K}^{-1}$ , while the CCSD(T) calculation gives a low-frequency vibration of  $401.1 \text{ cm}^{-1}$  and an entropy of  $65.9 \text{ cal mol}^{-1} \text{ K}^{-1}$ . All DFT calculations presented in Table S2 dramatically underestimate the lowest vibrational frequency of the *syn* conformation of urea, compared to CCSD(T) calculations. Large amplitude vibrations of urea in the gas phase have been reported and analyzed using *ab initio* calculations in the literature.<sup>34</sup> Complex behaviors were highlighted due to  $\text{NH}_2$  torsion and inversion motions, which led to the use of a variational treatment based on a 4D model to simulate the far infra-red spectrum of gas-phase urea. We note here that the lowest vibrational frequency measured in Ar-matrix is  $445.1 \text{ cm}^{-1}$ . DFT values for the *syn* conformer are therefore erroneous and we used the CCSD(T)/cc-pVTZ level of theory to calculate the partition functions of urea, using a multi-structural approach ( $C_2$  and  $C_s$  conformers included in the total RRHO partition function). At the CCSD(T)/CBS//CCSD(T)/cc-pVTZ level of calculation, the *anti* conformation ( $C_2$ ) lies  $1.3 \text{ kcal mol}^{-1}$  below the *syn* ( $C_s$ ) conformation, at 0 K and our computed value of standard entropy for urea is  $66.0 \text{ cal mol}^{-1} \text{ K}^{-1}$ .

For all the other molecular structures studied in the work, the issue with DFT computed low-frequency vibrational modes in *syn* urea was not encountered. Indeed, the *syn* conformations

in alkyl- and phenyl-ureas were not found to be minima of the PES, at all the envisaged levels of theories (DFT and MP2 levels). M06-2X calculations have therefore been performed for the calculation of the partition functions, with a scaling factor of 0.97 for the vibrational frequencies.<sup>24</sup>

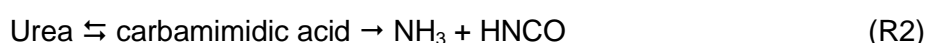
Canonical rate constants were computed and fitted with an Arrhenius-Kooij form:  $k = AT^n \exp\left(-\frac{E}{RT}\right)$ , for temperatures ranging from 500 to 2000K. A transmission coefficient involving a one-dimensional asymmetric Eckart potential has been systematically computed for reactions involving H-atom transfers. All of these calculations were performed by means of the ThermRot software.<sup>35</sup>

Pressure effects have been investigated for the thermal decomposition of urea by means of the Master Equation System Solver<sup>36</sup> code (MESS).<sup>37</sup> In these calculations, nitrogen (N<sub>2</sub>) was chosen as the buffer gas. The Lennard-Jones parameters of urea have been computed based on the relationships given by Tee et al.<sup>38</sup> with a boiling point, critical temperature and pressure equal, respectively, to 482 K, 705 K and 89 atm.<sup>39</sup>

### 3. Results and discussion

#### 3.A Thermal decomposition of urea

We recently proposed a gas-phase kinetic model for urea pyrolysis that explained the formation routes of solid deposits that perturb the post-combustion reduction of NO<sub>x</sub> processes.<sup>17</sup> Our kinetic model included the two initial decomposition pathways of urea demonstrated in the literature<sup>18, 19, 40</sup>, both yielding HNCO and NH<sub>3</sub>:



Reaction (R1) is the direct deamination and reaction (R2) first involves an acid intermediate formation followed by a deamination (see Figure 3). It can be noted that we showed that carbamimidic acid formation is at the origin of solid deposit compounds.<sup>17</sup>

In this work we explored other possible decomposition pathways on the PES of urea unimolecular decomposition routes, including initial bond fissions, and used the results as a reference for the decomposition of larger urea-derivatives. Our computational results show that neither initial bond fissions in urea or carbamimidic acid (Figure S1) nor alternative pericyclic reactions (Figure S2) cannot compete with reactions (R1) and (R2). It appears that urea mainly decomposes by two pathways: one involving direct deamination and the other involving a two-step deamination via the carbamimidic acid, urea's tautomer. Since carbamimidic acid only reacts according to reactions (R2), we performed a quasi-stationary state approximation (QSSA) on this species to simplify the reaction scheme and to compute the corresponding rate constant (Fig. 2a and 2b).

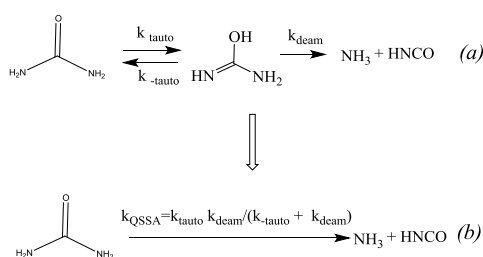


Figure 2: QSSA performed on the carbamimidic acid for the two steps deamination. (a) Initial reaction scheme.

(b) Simplified reaction scheme

Figure 3 depicts the values of the high-pressure rate constants for the two main pathways: direct  $\text{NH}_3$  elimination ( $k_{\text{direct}}$ ) and formation of the carbamimidic acid intermediate ( $k_{\text{QSSA}}$ ). The geometries and partition functions of the transition state structures for the direct deamination and the tautomerization are computed at the CCSD(T)/cc-pVTZ level of theory. This was required for the rate coefficient calculation to remain consistent with the multi-structural treatment of urea's partition function. All the other rate coefficients of the reactions of Figure 3 were computed with the ThermRot software<sup>15</sup>, based on CCSD(T)/CBS/M06-2X/6-311++G(3df,2p) calculations. Computed high-pressure limit rate constants can be found in Table S4.

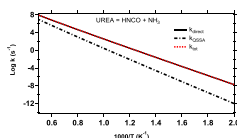


Figure 3: Canonical rate constants of direct (solid black line) and two-step deamination (QSSA, dashed black line).

Figure 3 shows that direct deamination is preponderant for temperatures ranging from 500K to 2000K. The ratio of direct deamination over the two-step deamination rate constants ranges between  $10^4$  at 500K and 9 at 2000 K. In fact, the reverse formation of urea from carbamimidic acid (with the rate constant  $k_{-tauto}$ ) is the most favorable pathway from a PES point of view, as shown in Figure S2. Accordingly, the rate constant  $k_{deam}$  is negligible, in a large temperature range, compared to  $k_{-tauto}$  and the QSSA rate constant becomes (eq.1):

$$k_{QSSA} = \frac{k_{tauto} k_{deam}}{k_{-tauto} + k_{deam}} \approx \frac{k_{tauto} k_{deam}}{k_{-tauto}} = K_{eq}^{tauto} k_{deam} \quad (\text{eq.1})$$

where  $K_{eq}^{tauto}$  represents the equilibrium constant of the tautomerization reaction. Even if  $k_{deam}$  is higher than the value obtained for the direct reaction of deamination, the equilibrium constant lowers the value of  $k_{QSSA}$  and then disadvantages the two-steps deamination process.

The pressure effects on the rate coefficients of decomposition of urea were also probed. The calculation was carried out using the MESS code of the PAPR suite.<sup>36, 37</sup> The main objective of these master equation simulations is to probe the importance of fall-off on the unimolecular decomposition of urea. Therefore, the geometries and vibrational frequencies of the well, transition state structures and products (for reactions R1 and R2) were taken from CCSD(T)/CBS//M06-2X/6-311++G(3df,2pd) calculation results. Internal rotations were treated with the 1D-HR approach and tunneling was computed with the Eckart method, as implemented in MESS.<sup>36</sup>

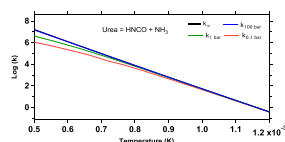


Figure 4: Pressure effect for the deamination reaction of urea. Both direct and two-step deamination are considered in the master equation simulation.  $k$  is in  $s^{-1}$ .

Figure 4 shows that pressure effect is relatively weak over a large temperature range. A factor of 2 is reached at 1700K between the high-pressure limit and the 1 bar rate coefficient. Since urea derivatives are much heavier molecules, we assumed that the pressure dependence of the rate constants of alkyl- and phenyl-urea can be neglected.

### 3.B Urea derivatives thermal decomposition pathways

Urea is the simplest molecule belonging to the urea-derivatives family. However, the most widespread ureas always feature substituents linked to the N-atoms, as depicted in Table 1. In order to establish reaction rate rules for the thermal decomposition of these types of urea-derivatives, as a function of the different substituents, the unimolecular decomposition of all structures presented in Table 4 were considered in our work.

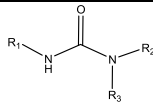
Table 4. General structures used to establish reaction rate rules for urea-derivatives thermal decomposition.  $R_n$  substituents are alkyl or phenyl groups.

		<i>Acceptor Group</i>		
<i>Transferred H-atom</i>		$N_{\text{primary}}$	$N_{\text{secondary}}$	$N_{\text{tertiary}}$
$H_{\text{primary}}$				
$H_{\text{secondary}}$				

As shown in Table 1,  $R_n$  are alkyl or phenyl groups and two urea-derivatives families can be defined: alkylureas and phenylureas. We explored the unimolecular decomposition pathways of about 10 urea-derivatives. First, we calculated their enthalpies of formation and bond

dissociation energies. Table 5 contains all the computed isodesmic enthalpies of formation for the urea-derivatives studied in this work.

Table 5. Isodesmic enthalpies of formation of urea derivatives calculated at the CCSD(T)/CBS and CBS-QM06 levels of theory (this work) and experimental or tabulated enthalpies<sup>6</sup>. MAD for our calculations is computed from 3 isodesmic reactions (see Table S5).

	R1	R2	R3	$\Delta_f H^\circ$ this work (kcal mol <sup>-1</sup> )	Literature	
					$\Delta_f H^\circ$ exp (kcal mol <sup>-1</sup> )	reference <sup>6</sup> (kcal mol <sup>-1</sup> )
Urea	H	H	H	-56.3 ± 0.3 <sup>a</sup>	-56.28 ± 0.29	-55.89 ± 0.84
Methylurea	CH <sub>3</sub>	H	H	-55.5 ± 0.8 <sup>a</sup>	-55.43 ± 0.35	-54.89 ± 0.84
N,N-dimethylurea	H	CH <sub>3</sub>	CH <sub>3</sub>	-53.8 ± 1.0 <sup>a</sup>	-53.92 ± 0.19	-53.84 ± 0.84
N,N'-dimethylurea	CH <sub>3</sub>	H	CH <sub>3</sub>	-54.2 ± 1.0 <sup>a</sup>	-53.75 ± 0.31	-54.06 ± 0.84
Trimethylurea	CH <sub>3</sub>	CH <sub>3</sub>	CH <sub>3</sub>	-51.8 ± 0.5 <sup>a</sup>	no data available	-52.96 ± 1.1
Ethylurea	C <sub>2</sub> H <sub>5</sub>	H	H	-61.7 ± 0.5 <sup>a</sup>	-61.78 ± 0.26	-62.28 ± 0.83
i-Propylurea	C <sub>3</sub> H <sub>7</sub>	H	H	-68.4 ± 0.5 <sup>a</sup>	-69.65 ± 0.33	-70.6 ± 0.83
t-Butylurea	C <sub>4</sub> H <sub>9</sub>	H	H	-74.3 ± 0.5 <sup>a</sup>	-75.74 ± 0.23	-78.32 ± 0.83
Phenylurea	C <sub>6</sub> H <sub>5</sub>	H	H	-26.4 ± 1.0 <sup>b</sup>	no data available	-24.76 ± 0.96
N-methyl-N'-phenylurea	C <sub>6</sub> H <sub>5</sub>	CH <sub>3</sub>	H	-26.4 ± 1.0 <sup>b</sup>	no data available	no data available
N,N-dimethyl-N'-phenylurea	C <sub>6</sub> H <sub>5</sub>	CH <sub>3</sub>	CH <sub>3</sub>	-25.0 ± 1.0 <sup>b</sup>	no data available	no data available

<sup>a</sup> CCSD(T)/CBS ; <sup>b</sup> CBSQ-M06

Most of the enthalpies of formation calculated in this work agree with experimental data, within their respective uncertainty ranges. Two new enthalpies of formation for urea-derivatives have been calculated here: for N-methyl-N'-phenylurea and N,N-dimethyl-N'-phenylurea. Computed standard entropies and heat capacities and NASA polynomials are given in Table S6. Bond dissociation energies of all the alkylureas and phenyl-ureas studied here were also computed and are presented in Figure 5.

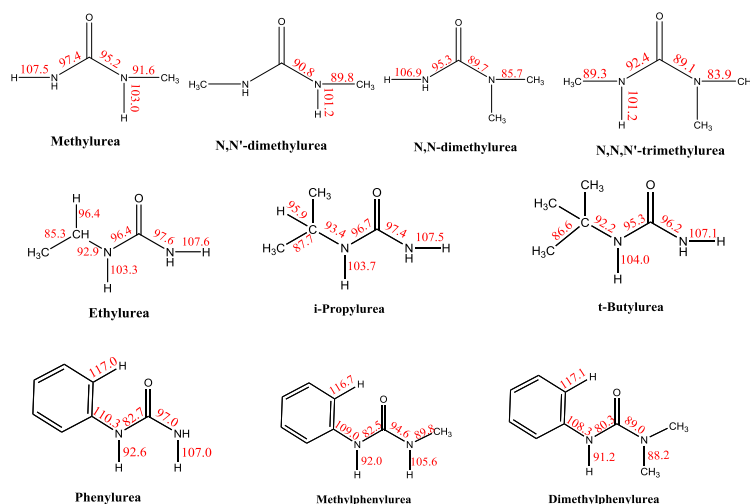


Figure 5 : Bond dissociation energies (in kcal mol<sup>-1</sup>) of urea derivatives computed at the CBS-QB3 level of calculation.

Table 6 presents the computed BDEs of all urea derivatives as a function of the natures of the bonds. It is interesting to note that N-H<sub>primary</sub> bonds have consistent BDEs (mean value of 107.3 kcal mol<sup>-1</sup>, see Table 6), which is 3.7 kcal mol<sup>-1</sup> below the experimental value in urea. We will see below that the presence of a methyl group on the opposite N-atom, with respect to the central CO group has an effect on the BDEs of a given N-atom. It can be noted that the BDE of a N-H<sub>primary</sub> bond is close to the value in NH<sub>3</sub> (107.6 kcal mol<sup>-1</sup>).<sup>41</sup> An experimental BDE value of 99.1 kcal mol<sup>-1</sup> was reported for the C-N bond in CH<sub>3</sub>CONH<sub>2</sub>, which is slightly higher than our computed BDEs for NR<sub>1</sub>R<sub>2</sub>CONH<sub>2</sub> (with R<sub>1</sub> and R<sub>2</sub> = H, CH<sub>3</sub> or phenyl) which have a mean value of 96.8 kcal mol<sup>-1</sup>. This difference of 2.3 kcal mol<sup>-1</sup> can be explained by the possibility of electronic resonance induced by the presence of a NR<sub>1</sub>R<sub>2</sub> group in urea derivatives instead of a CH<sub>3</sub> group in CH<sub>3</sub>CONH<sub>2</sub>.

Table 6. Bond dissociation energies of urea derivatives (kcal mol<sup>-1</sup>). CBS-QB3 calculations.

	Methyl urea	N,N'-(CH <sub>3</sub> ) <sub>2</sub> urea	N,N-(CH <sub>3</sub> ) <sub>2</sub> urea	N,N,N'-(CH <sub>3</sub> ) <sub>3</sub> urea	Ethyl urea	i-C <sub>3</sub> H <sub>7</sub> urea	t-butyl urea	Phenyl urea	Methyl phenyl urea	Dimethyl Phenyl urea	Mean ± MAD <sup>b</sup>
N-H <sub>primary</sub>	107.5	-	106.9	-	107.6	107.5	107.1	107.0	-	-	107.3 ±0.3
N-H <sub>secondary</sub>	103.0	101.2	-	101.2	103.3	103.7	104.0	-	105.6	-	103.1 ±1.5
N-H <sub>benzyl,secondary</sub>	-	-	-	-	-	-	-	92.6	92.0	91.2	91.9 ±0.5
N(CO)(H)-R <sub>n</sub> <sup>d</sup>	91.6	89.8	-	89.3	92.9	93.4	92.2	-	89.8	-	91.3 ±1.4
N(CO)(H)-phenyl	-	-	-	-	-	-	-	110.3	109.0	108.3	109.2 ±0.7
N(CO)(CH <sub>3</sub> )-CH <sub>3</sub>	-	-	85.7	83.9	-	-	-	-	-	88.2	85.9 ±1.5
NH <sub>2</sub> -CO	97.4	-	95.3	-	97.6	97.4	96.2	97.0	-	-	96.8 ±0.7
N(H)(R <sub>n</sub> )-CO <sup>d</sup>	95.2	90.8	-	92.4	96.4	96.7	95.3	-	94.6	-	95.1 ±1.1
N(H)(phenyl)-CO	-	-	-	-	-	-	-	82.7	82.5	80.3	81.8 ±1.0
N(CH <sub>3</sub> ) <sub>2</sub> -CO	-	90.8	89.7	89.1	-	-	-	-	-	89.0	89.9 ±0.9
Phenyl-H	-	-	-	-	-	-	-	117.0	116.7	117.1	116.9 ±0.2

<sup>a</sup> R<sub>n</sub> is the alkyl group in the given alkylurea, <sup>b</sup> Mean Absolute Deviation

For a given type of bond, the results presented in Table 6 show a good consistency. All the MAD falls within the uncertainty limits of the CBS-QB3 calculations. It can be noted that the replacement of a methyl- with an ethyl-, *i*-propyl- or t-butyl- group has only a slight effect on the BDE, even for the N(CO)(H)-R<sub>n</sub> configurations, where the nature of the alkyl radicals formed are different (primary, secondary, tertiary and quaternary radicals). All these structures feature a -NH<sub>2</sub> group on one side of the central C=O group and a -N(H)-R<sub>n</sub> group on the other side. If H-atoms of the -NH<sub>2</sub> group are substituted by 1 or 2 methyls or by a phenyl group, there is a decrease in the N(CO)(H)-R<sub>n</sub> bond dissociation energy on the other side of the C=O group (around 89.6 kcal mol<sup>-1</sup>). It seems that non-bonded interactions are



playing a role on the BDEs for  $N(\text{CO})(\text{H})-\text{R}_n$  bonds. This phenomenon is also observed in  $N(\text{H})(\text{R}_n)-\text{CO}$ ,  $N(\text{CO})(\text{CH}_3)-\text{CH}_3$ ,  $\text{NH}_2-\text{CO}$  and  $\text{N}-\text{H}_{\text{secondary}}$  bonds, where the presence of a substituent on the opposite N-atom group systematically decreases the BDE. This conclusion needs to be verified against largest set of molecular structures, but this is beyond the scope of this work.

Known trends in BDEs are also observed in our calculations:  $\text{N}-\text{H}_{\text{primary}} > \text{N}-\text{H}_{\text{secondary}}$ ,  $\text{N}-\text{H}_{\text{benzyl}}$  and N-C bonds have lower BDEs than comparable non-benzyl bonds by 11.2 and 13.3 kcal mol<sup>-1</sup>, respectively.

All the BDEs remain high compared to the energy barrier of the direct deamination in urea (48 kcal mol<sup>-1</sup>), even for lowest C-N benzyl bond (80.3 kcal mol<sup>-1</sup>). The radical pathways can therefore be neglected in the unimolecular decomposition of urea derivatives and our kinetic study focused on the pericyclic eliminations.

The PES of unimolecular decomposition of urea (Figure S2) and the associated rate coefficients (Figure 3) showed that the direct  $\text{NH}_3$  elimination is the most favored pathway between 500 and 2000 K. The influence of the substituents on this decomposition pathway is first assessed here.

The presence of substituents in urea derivatives breaks the symmetry of the pericyclic reactions (except for N,N'-dimethylurea) and double the possible pathways. Figure 6 presents the computed PES of pericyclic reactions of methylurea.

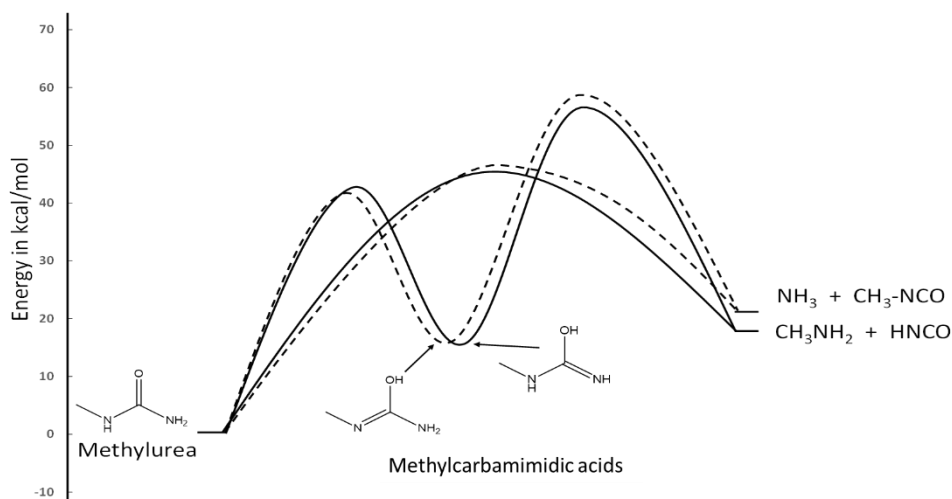


Figure 6. Methylurea pericyclic reactions computed at the CCSD(T)/CBS level of theory.

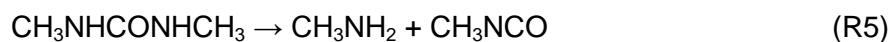
Solid line: 4- $H_pN_s$  elimination; dashed line: 4- $H_sN_p$  elimination.

As seen in Figure 6, a H-atom can be transferred from the  $-NH_2$  group (solid line) or from the  $-N(H)CH_3$  group (dashed line) both through a direct elimination or via the formation of a carbamimidic acid. As in urea, the elimination reaction through the carbamimidic acid intermediate can be neglected because the reverse reaction of the intermediate to methylurea is much easier than its decomposition. Two direct elimination reactions can therefore be written for methylurea:



In (R3), a secondary H-atom ( $H_s$ ) is transferred to a primary  $-NH_2$  acceptor group ( $N_p$ ) through a 4-membered transition state structure. We will note this reaction as “4- $H_sN_p$ ”. (R4) is the inverse reaction of (R3): 4- $H_pN_s$ . The CCSD(T)/CBS calculations predict that the energy barrier of (R3) ( $47.4 \text{ kcal mol}^{-1}$ ) lies only  $0.6 \text{ kcal mol}^{-1}$  above the one for (R4) ( $46.8 \text{ kcal mol}^{-1}$ ). The nature of the transferred H-atom (p or s) varies with the nature of the acceptor group (s or p) and seem to yield nearly unchanged energy barrier. Note that in urea, the reaction is 4- $H_pN_p$  and feature a critical energy of  $48.8 \text{ kcal mol}^{-1}$ . Going from 4- $H_pN_p$  to 4- $H_sN_p$ , the energy barrier decreases by  $1.4 \text{ kcal mol}^{-1}$ .

N,N'-dimethylurea features two -N(H)CH<sub>3</sub> groups on each side of the central carbonyl and decomposes through the following pericyclic reaction:



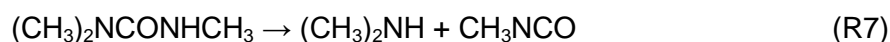
The CH<sub>3</sub>NH<sub>2</sub> elimination in (R5) can be classified as 4-H<sub>s</sub>N<sub>s</sub> and faces an energy barrier of 44.9 kcal mol<sup>-1</sup>, which is 2.5 kcal mol<sup>-1</sup> below the one for the 4-H<sub>s</sub>N<sub>p</sub> reaction (R3).

N,N-dimethylurea has two methyl groups linked to a N-atom and two H-atom linked to the other N-atom. Only one direct elimination reaction is possible:



This elimination belongs to the 4-H<sub>p</sub>N<sub>t</sub> class and faces an energy barrier of 41.9 kcal mol<sup>-1</sup>. A tertiary acceptor N-atom in the reaction leads to a lower energy barrier compared to a secondary (4-H<sub>p</sub>N<sub>s</sub>), with a strong decrease of energy of 5 kcal mol<sup>-1</sup>.

Similarly to N,N'- and N,N-dimethylurea, trimethylurea can only decompose through one elimination reaction,



which is a 4-H<sub>s</sub>N<sub>t</sub> reaction type, with a computed energy barrier of 39.9 kcal mol<sup>-1</sup>. This is the lowest computed energy barrier for this type of pericyclic reaction in urea-derivative. The increase in the substitution of the N<sub>acceptor</sub> group systematically decreases the energy barrier. Table 7 summarizes the computed results for all the possible 4-H<sub>x</sub>N<sub>y</sub> reactions.

Table 7. Energy barriers at 0K (kcal mol<sup>-1</sup>) calculated at the CCSD(T)/CBS level of theory for the 4-H<sub>x</sub>N<sub>y</sub> reactions in alkylurea derivatives.

<i>Transferred H-atom</i>	<i>Acceptor Group</i>		
	N <sub>primary</sub>	N <sub>secondary</sub>	N <sub>tertiary</sub>
H <sub>primary</sub>	48.8	46.8	41.9
H <sub>secondary</sub>	47.4	44.9	39.9

As expected, the energy barriers for the transfer of a secondary H-atom are systematically lower than that for a H<sub>primary</sub>, by about 2 kcal mol<sup>-1</sup>. The increase in the substitution of the

$N_{\text{acceptor}}$  group systematically decreases the energy barrier, by about 2 kcal mol<sup>-1</sup> when the substitution is going from  $N_{\text{primary}}$  to  $N_{\text{secondary}}$  and by 5 kcal mol<sup>-1</sup> for  $N_{\text{secondary}}$  to  $N_{\text{tertiary}}$ . Despite their complexity, these effects seem to be able to be rationalized in the form of structure-reactivity relationships for alkylureas. From Table 7, we see that this type of correlations can be determined from urea and methyl-ureas. However, in order to use these compounds to propose new reaction rate rules, we need to verify if new favorable decomposition routes are created as the size of the alkyl group increases. We therefore computed the PES of ethyl- and *i*-propyl-urea. Figure 7 presents the PES computed for ethyl-urea.

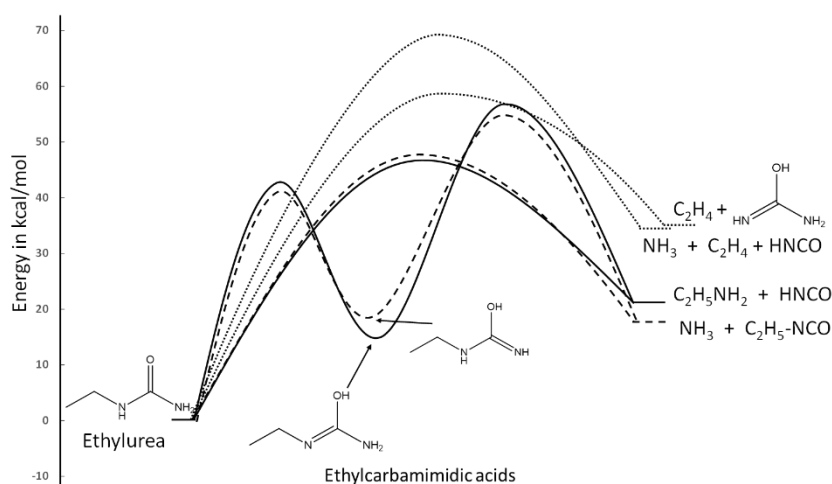


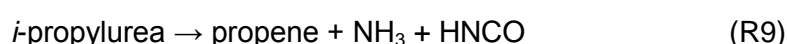
Figure 7. Ethylurea unimolecular decomposition routes, computed at the CCSD(T)/CBS level of theory.

4- $H_pN_s$  transfer: solid line; 4- $H_sN_p$  transfer: dashed line; 6-membered ring transition states: dotted line.

The  $C_2H_5$  group in ethyl-urea allows three possible additional pericyclic reactions. The first one is the elimination of  $C_2H_4$  through a 4-membered TS structure, in which an H-atom from the methyl group is transferred to the secondary N-atom yielding ethylene and urea (not depicted in Figure 7). Our calculation shows that this reaction features the highest energy barrier of the PES (77.9 kcal mol<sup>-1</sup>) and can be neglected. The two other possible pericyclic reactions occurred through 6-membered cyclic TS and are displayed in Figure 7 (dotted lines). The first reaction involves the transfer of a H-atom from the methyl group to the primary N-atom and leads to  $C_2H_4$ ,  $NH_3$  and  $HNCO$  and faces an energy barrier of 69 kcal mol<sup>-1</sup>, which is 25 kcal mol<sup>-1</sup> above the direct deamination. The other six-center reaction

involves the transfer of a hydrogen from the methyl group to the oxygen atom, yielding C<sub>2</sub>H<sub>4</sub> and carbamimidic acid. The computed energy barrier is 59 kcal/mol, which is 15 kcal/mol above the direct deamination.

The increase in the alkyl chain length leads to additional pericyclic reactions but with energy barriers lying at least 15 kcal mol<sup>-1</sup> above the direct deamination routes. Indeed, similar results were found for *i*-propylurea with the following reactions:



where all these reactions can be classified as alkene elimination. The computed energy barriers for (R8) and (R9) are 59.6 and 69.3 kcal mol<sup>-1</sup>, respectively.

These 6-center pericyclic pathways can be neglected in the unimolecular decomposition of alkylureas and rate rules for their thermal decomposition only involve the 4-center deamination. Moreover, if new radical initiations can appear, due to the alkyl chains, the corresponding BDEs remain largely higher than the energy barriers involved in the concerted reactions and can be neglected. These rate rules for the thermal decomposition of alkyl urea are given in Table 8.

Table 8. High-pressure limit rate constants ( $k = A \times T^n \times \exp(-E/RT)$ ) calculated at the CCSD(T)/CBS level of theory for the 4-H<sub>x</sub>N<sub>y</sub> reaction rate rule of alkylurea derivatives.

	A (s <sup>-1</sup> )	n	E (cal mol <sup>-1</sup> )
4-H <sub>p</sub> N <sub>p</sub>	1.08×10 <sup>8</sup>	1.453	45004
4-H <sub>p</sub> N <sub>s</sub>	7.25×10 <sup>6</sup>	1.488	43826
4-H <sub>p</sub> N <sub>t</sub>	7.62×10 <sup>5</sup>	1.985	38997
4-H <sub>s</sub> N <sub>p</sub>	6.06×10 <sup>7</sup>	1.188	44547
4-H <sub>s</sub> N <sub>s</sub> <sup>a</sup>	2.46×10 <sup>8</sup>	1.187	41878
4-H <sub>s</sub> N <sub>t</sub>	2.00×10 <sup>6</sup>	2.132	37314

<sup>a</sup> This rate constant is for the general case where the reactant has no external symmetry. If the reactant has an external symmetry of 2, like N,N'-dimethylurea, the rate constant has to be multiplied by 2.

The rate rules proposed in Table 8 can be applied to any alkylurea with a primary or a secondary H-atom. If a primary H-atom is involved, the reaction always yields isocyanic acid

and an amine and can be written as  $\text{NH}_2\text{CONR}_1\text{R}_2 \rightarrow \text{R}_1\text{R}_2\text{NH} + \text{HNCO}$ . In the case of a secondary H-atom, the decomposition reaction is  $\text{NHR}_3\text{CONR}_1\text{R}_2 \rightarrow \text{R}_1\text{R}_2\text{NH} + \text{R}_3\text{NCO}$  and leads to the formation of an amine and an alkyl isocyanate. The proposed reaction rate rule can be applied for gas-phase thermal decomposition of alkyl-ureas, with or without oxygen, for temperature ranging between 500 and 2000 K. As an example, Figure 8 presents the evolution of the rate coefficient for a secondary H-atom transfer as a function of the substituents on the N-atom of the acceptor side.

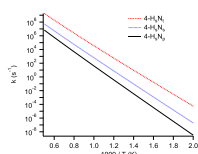


Figure 8 : Rate coefficients for the 4-H<sub>s</sub>N<sub>y</sub> rate rule in alkylureas

The trends observed in activation energies in Table 7 are also found in the computed rate parameters: the rate increases with the degree of branching on the acceptor N-atom. For a secondary H-atom transferred, going from a primary to a secondary acceptor N-atom leads to an increase of the rate constant by a factor of 15 at 1000 K. A further increase from N<sub>s</sub> to N<sub>t</sub> yield to a factor of 55 at 1500 K. The level of branching of the acceptor N-atom is therefore a very sensitive parameter on the rate of decomposition of alkylureas.

In a previous study, we showed that the formation of deposits during the pyrolysis of condensed phase urea is due to the formation of the carbamimidic acid tautomer of urea.<sup>17</sup> This acid tautomer can also be formed in any alkylurea that bears a primary or secondary H-atom. Since these reactions can be neglected in the thermal decomposition of gas-phase alkylureas, the rate coefficients are not presented here but are given in Table S7.

As shown in Table 1, the substituents in urea-derivatives can also be phenyl groups that create benzylic bonds. We therefore computed the PES of phenylurea unimolecular decomposition and established reaction rate rules for these compounds, based on N-methyl-

N'-phenylurea and N,N-dimethyl-N'-phenylurea. Figure 9 depicts the PES computed for phenyl-urea.

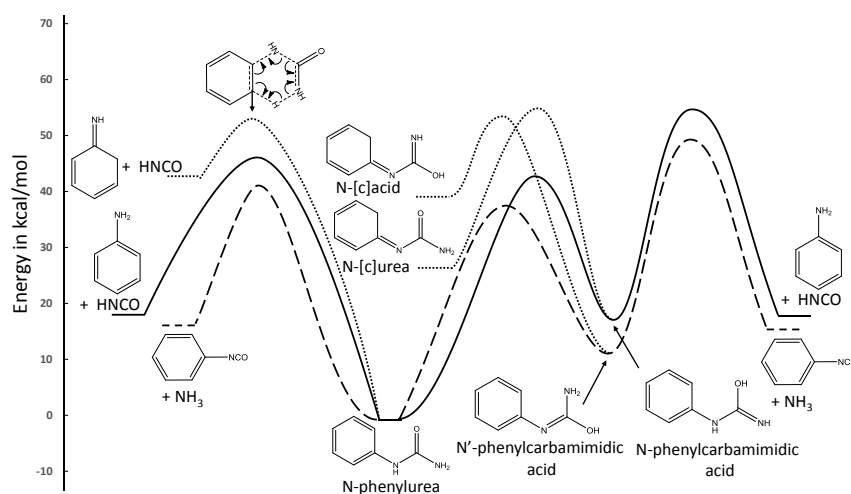


Figure 9. Unimolecular decomposition of phenyl-urea computed at the CBS-QM06 level of theory.

First, it is observed that similar reactions to those obtained for alkyl-urea are involved (dashed and solid lines): the direct elimination of HNCO or phenyl-isocyanate ( $C_6H_5-NCO$ ) and the two-step elimination via the formation of tautomer intermediates N'- and N-phenylcarbamidic acids. The energy barriers for these reactions are similar to that computed for alkyl-urea and it appears from the PES that the direct elimination will be favored over the two-step elimination. This is further confirmed from our calculations using the QSSA approximation on these tautomers (using rate coefficients given in Table 9 and Table S7 and equation (1)). The first direct elimination involves the transfer of a primary H-atom yielding aniline ( $C_6H_5-NH_2$ ) and HNCO and faces an energy barrier of  $47.6 \text{ kcal mol}^{-1}$  at the CBSQ-M06 level of calculation. This reaction belongs to the  $4-H_pN_s$  reaction rule and the computed barrier is close to that calculated for alkyl-urea ( $46.8 \text{ kcal mol}^{-1}$ ). Here, the formation of a phenyl isocyanate leads to an energy barrier similar (within the uncertainty limits) to that of an alkyl isocyanate and the presence of a phenyl instead of a methyl does not seem to affect the critical energy. The other direct elimination yields  $NH_3$  and phenyl isocyanate and involves the transfer of a secondary benzylic H-atom ( $4-H_{s\text{-benzyl}}N_p$ ). The computed energy barrier is  $43.8 \text{ kcal mol}^{-1}$  and lies  $3.6 \text{ kcal mol}^{-1}$  below the  $4-H_sN_p$  critical

energy in alkyl-urea. The benzylic stabilization effect is also observed in the isomerization reaction yielding N'-phenylcarbamidic acid, transfer of the benzylic H-atom, that occurs with an energy barrier of 39.6 kcal mol<sup>-1</sup>. A similar reaction involving an alkyl secondary H-atom in methyl-urea has a critical energy of 43.6 kcal mol<sup>-1</sup>. HNCO and phenyl-NCO eliminations in N- and N'-phenylcarbamidic acids faces energy barriers of 57.0 and 51.7 kcal mol<sup>-1</sup>, respectively.

In addition to these decomposition routes, the presence of the phenyl group allows another pericyclic reaction in N-phenylurea, through a 6-membered ring transition state structure (dotted line in Figure 9), yielding a tautomer of aniline (cyclohexa-2,4-dien-1-imine) and HNCO. This elimination faces an energy barrier of 54.8 kcal mol<sup>-1</sup>, 11 kcal mol<sup>-1</sup> above the lowest 4-center direct deamination barrier and can therefore be neglected between 500 and 1500 K. The phenyl group also allows additional 6-center isomerization pathways for N- and N'- phenylcarbamidic acids, leading N-[(1E)-cyclohexa-2,4-dien-1-ylidene]urea and N-[(1E)-cyclohexa-2,4-dien-1-ylidene]carbamidic acid (noted N-[c]X in Figure 12), but their formation faces high energy barriers (55.7 and 53.7 kcal mol<sup>-1</sup>, respectively) compared to 4-center direct eliminations.

The computed PESs for N-methyl-N'-phenylurea and N,N-dimethyl-N'-phenylurea are given in Figure S3. A behavior similar to that of alkyl urea and phenyl urea is observed: the direct 4-center eliminations are favored over all other pathways. For all the considered phenyl-ureas, the direct elimination of aniline belongs to the 4-H<sub>x</sub>N<sub>s</sub> rate rule defined for the alkyl-ureas. The presence of a phenyl group creates a new rate rule, in which a secondary benzyl H-atom is transferred to a N-atom which can be primary, secondary or tertiary. High-pressure limit rate coefficients for this additional rate rule are given in Table 9.

Table 9. High-pressure limit rate constants ( $k = A \times T^n \times \exp(-E/RT)$ ) calculated at the CBSQ-M06 level of theory

reaction	A (s <sup>-1</sup> )	n	E (cal mol <sup>-1</sup> )	for the 4-H <sub>s</sub> -benzylN <sub>y</sub> rate rule of phenylurea
4-H <sub>s</sub> -benzylN <sub>p</sub>	4.92×10 <sup>7</sup>	1.411	41175	
4-H <sub>s</sub> -benzylN <sub>s</sub>	8.23×10 <sup>7</sup>	1.441	39292	
4-H <sub>s</sub> -benzylN <sub>t</sub>	3.30×10 <sup>5</sup>	2.255	33749	



derivatives.

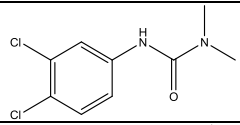
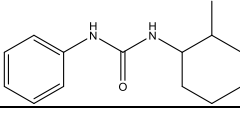
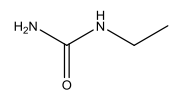
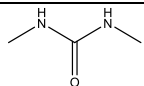
At 1000 K, the ratio between the computed rate constants for 4-H<sub>s</sub>-benzylN<sub>s</sub> and 4-H<sub>s</sub>N<sub>s</sub> (see Table 8) is a factor of 7. As expected, when the transferred H-atom is benzylic, the rate constant is systematically higher compared to a hydrogen atom bonded to an alkyl group. For a phenyl-urea, the rate constants of Table 9 are associated with the reaction  $\text{RPhNHCONR}_1\text{R}_2 \rightarrow \text{R}_1\text{R}_2\text{NH} + \text{RPh-NCO}$ .

Urea and some of its derivatives start to decompose in their condensed phase and the use of gas-phase rate rules to describe these complex heterogeneous phenomena probably induce higher uncertainties on the predicted rate of decomposition. In a recent study,<sup>17</sup> we qualitatively simulated the experimental results of the pyrolysis of a solid urea sample performed by Schaber et al.<sup>12</sup> using a gas phase reaction mechanism and a homogenous batch reactor. The simulation results show that the products branching ratios predicted by the gas phase model agree with the experiments but that simulation temperatures have to be artificially increased by 180 K in the simulations to reproduce the experimental conversion of urea. This means that the condensed phase, heterogeneous pyrolysis of urea is faster than in the gas phase. This difference in reactivity can be due to catalytic effects in the condensed phase and/or to the use of a too simple reactor model to simulate experiments not well defined kinetically. Further work needs to be done to determine the effects of the changes in the state of matter on these decomposition rate rules. Based, on our work on urea, and from a process safety point of view, our gas-phase rate rules are expected to give the lower limit of the decomposition rate constant of condensed phase ureas.

To illustrate the rate rules for the thermal decomposition of alkyl- and phenyl-ureas (Tables 8 and 9), they were applied on ureas produced industrially on a large scale for fine chemicals

or drugs production<sup>42</sup> (alkyl-ureas) or as pesticides<sup>43, 44</sup> (phenyl-ureas). Table 10 depicts the selected ureas used for the application of rate rules.

Table 10. Application of thermal decomposition reaction rules of alkyl- and phenyl-ureas of interest.

Name	Structure	Uses	Applicable reaction rules
Diuron		Herbicide, algicide	$4\text{-H}_s\text{-benzylN}_i:$ $\text{RPhNHCONR}_1\text{R}_2 \rightarrow \text{R}_1\text{R}_2\text{NH} + \text{RPh-NCO}$
Siduron		Herbicide	$4\text{-H}_s\text{-benzylN}_s:$ $\text{PhNHCONHR}_1 \rightarrow \text{R}_1\text{NH}_2 + \text{Ph-NCO}$ & $4\text{-H}_s\text{N}_s:$ $\text{PhNHCONHR}_1 \rightarrow \text{Ph-NH}_2 + \text{R}_1\text{NCO}$
ethylurea		Polymer production	$4\text{-H}_s\text{N}_p:$ $\text{NH}_2\text{CONHR}_1 \rightarrow \text{NH}_3 + \text{R}_1\text{NCO}$ & $4\text{-H}_p\text{N}_s:$ $\text{NH}_2\text{CONHR}_1 \rightarrow \text{R}_1\text{-NH}_2 + \text{HNCO}$
N,N'-dimethylurea		Intermediate in the synthesis of fine chemicals, drugs, textile aids and herbicides	$4\text{-H}_s\text{N}_s:$ $\text{R}_1\text{NHCONHR}_2 \rightarrow \text{R}_1\text{NH}_2 + \text{R}_2\text{NCO}$

The first example taken from Table 10 is focused on siduron. Two decomposition pathways can be envisaged according to the reaction rules: siduron  $\rightarrow$  Ph-NCO + 2-methylcyclohexan-1-amine ( $4\text{-H}_s\text{-benzylN}_s$ ) and siduron  $\rightarrow$  aniline + 1-isocyanato-2-methylcyclohexane ( $4\text{-H}_s\text{N}_s$ ). Rate constants for the two reactions can be estimated with the reaction rate rules (Figure 10).

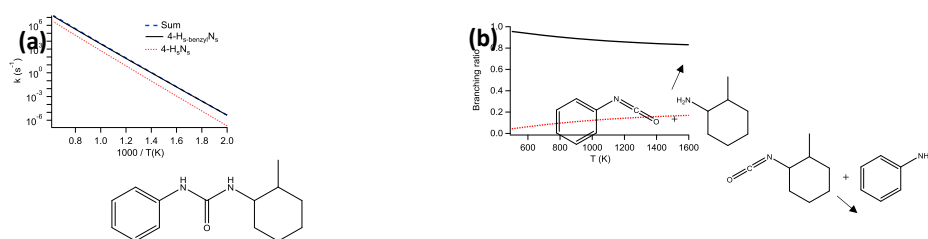


Figure 10: Application of thermal decomposition reaction rules to siduron (1-(2-Methylcyclohexyl)-3-phenylurea). (a): reaction rate constants; (b): relative branching fractions deduced from rate rules.

As expected, Figure 10a demonstrates that the transfer of the benzyl H-atom is favored over the alkyl one in siduron, by a factor ranging between 22 at 500 K and 5 at 1500 K. Computed branching ratios (Figure 10b) show that the predicted yield of Ph-NCO and 2-methylcyclohexan-1-amine is dominant over the temperatures considered (yields ranging

between 0.96 and 0.83 at 500 and 1500 K, respectively). The formation of aniline and 1-isocyanato-2-methylcyclohexane is negligible below 600 K but becomes significant at higher temperatures (0.1 – 0.16 branching ratio).

Comparisons between the kinetics of decomposition of two different phenylureas herbicides can also be achieved using the proposed reaction rate rules. Figure 11 depicts the decomposition kinetics of diuron and siduron.

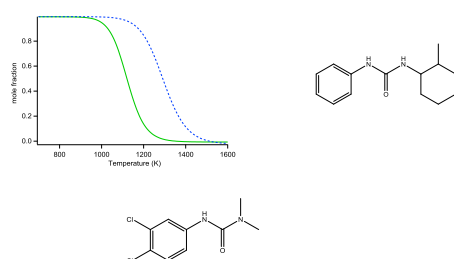


Figure 11: Comparison between the decomposition of diuron and siduron as a function of temperature using reaction rules given in Table 9 (total rate for siduron). Computed as a first-order reaction with 1  $\mu$ s residence time.

An important difference of reactivity is predicted, as diuron starts to decompose at 900 K while siduron thermal degradation begins at 1050 K. This temperature shift is due to a difference in the nature of the N-atom acceptor in the 4-center elimination: tertiary for diuron and secondary for siduron. Diuron decomposition solely yields dimethylamine and 1,2-dichloro-4-isocyanatobenzene.

Alkylureas thermal decomposition kinetics can also be estimated based on our reaction rate rules and, as an illustration, we estimated the branching ratio and compared the reactivity of the two alkylureas presented in Table 10: ethylurea and dimethylurea (Figure 12).

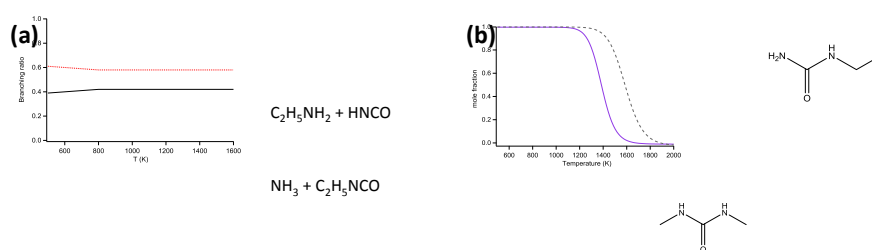


Figure 12: Application of thermal decomposition reaction rules to ethylurea and N,N'-dimethylurea. (a): branching ratios of decomposition products of ethylurea deduced from rate rules; (b): Comparison between the decomposition the two alkylureas as a function of temperature using reaction rules given in Table 9 (total rate for ethylurea). Computed as a first-order reaction with 1  $\mu$ s residence time.

Ethylurea decomposition products have almost constant yields over the studied temperature range, with values of 42% for the  $\text{NH}_3$  + ethyl-isocyanate channel and 58% for ethylamine + HNCO (Figure 12a). Both decomposition channels need to be considered for ethylurea. The comparison between the thermal degradation kinetics of ethyl- and N,N'-dimethylurea (Figure 12b) shows that the decomposition of N,N'-dimethyl urea occurs 200 K below that of ethylurea. Note that it is possible to rank the 4 urea derivatives of Table 10 by order of decreasing reactivity: diuron > siduron > N,N'-dimethylurea > ethylurea. To the best of our knowledge, this is the first time in the literature that such semi-quantitative comparisons can be made and this shows the interest of the proposed reaction rate rules.

The development of pyrolysis or combustion kinetic models for urea derivatives can be done using the proposed reaction rate rules. Our calculations show that these compounds will rapidly decompose by the 4-center pericyclic reactions, with energy barriers ranging from 38 to 47 kcal mol<sup>-1</sup>. A similar behavior was observed in the thermal decomposition of organophosphorous toxic compounds where, even at high temperatures, a 6-center pericyclic elimination (with an energy barrier around 40 kcal mol<sup>-1</sup>) is the only initial decomposition step, with no radical consumption of the reactant.<sup>45</sup> For these systems, and it also was observed for phosgene and diphosgene,<sup>46</sup> only the molecular fragments produced in the pericyclic reactions are oxidized under combustion conditions. Therefore, their combustion kinetic models can be written as a set of pericyclic reactions on top of detailed sub-mechanisms for their unimolecular decomposition products. This approach can be applied for alkyl- and phenyl-ureas where their pericyclic reactions will yield isocyanates and amines. The construction of urea derivatives kinetic models will need sub-mechanisms for these two families of compounds. If detailed chemical kinetic models for the combustion of amines are available in the literature<sup>47-51</sup>, it is not the case for isocyanates for which only HNCO sub-mechanisms are available.<sup>52</sup> Therefore, progresses in the understanding and

modeling of the kinetics of combustion of isocyanates remain to be done to be able to develop detailed chemical kinetic models for urea derivatives combustion and pyrolysis.

## 4. Conclusion

This study proposes reaction rate rules based on theoretical calculations for the thermal decomposition of urea derivatives belonging to the alkyl- and phenylureas families. First, the unimolecular decomposition routes of urea, the building block of all derivatives, were thoroughly explored and our results show that the  $\text{NH}_3 + \text{HNCO}$  elimination is the main decomposition route of urea. This elimination can take place in one step (direct elimination) or in two steps involving first an isomerization step followed by an elimination. Rate coefficients calculations and QSSA analysis showed that the two-steps elimination can be neglected compared to the direct elimination. Master equation simulations confirmed that the two-step elimination flux is negligible at different pressures and that pressure dependence of the direct elimination rate constant is very small. Bond dissociation energies were also computed for urea and showed that initial bond fissions are too high to compete with the 4-center direct elimination. Based on the detailed analysis of urea decomposition, the influence of alkyl and phenyl substituents on the decomposition routes and decomposition kinetics were investigated. These substituents were chosen because they are the ones most commonly found in ureas used in the industry. About 10 urea derivatives were considered and their thermochemical data, bond dissociation energies, PES of decomposition and associated kinetic data were systematically computed. When available, comparisons between experimental enthalpies of formation and our calculations showed a good agreement. Enthalpies of formation of several phenylureas are reported for the first time. Bond dissociation energies were systematically computed for all urea derivatives and showed a good consistency in BDEs for the same types of bond in the different molecules. The majority of these data are the first ones reported in the literature. For all alkyl- and phenylureas, the influence of the substituents on the possible decomposition pathways were assessed and our calculations showed that the direct 4-center elimination remains dominant for all the urea

derivatives. The products of their thermal degradation are always substituted amines and isocyanates. The set of urea derivatives studied allowed us to propose a reaction rate rule for their thermal decomposition based on the nature of transferred H-atom (primary or secondary / alkyl or benzyl) and the nature of the N-atom acceptor (primary, secondary and tertiary). As expected, the ranking of reactivity as a function of the nature of the H-atom is  $H_{s\text{-benzyl}} > H_{s\text{-alkyl}} > H_{p\text{-alkyl}}$ . The influence of the nature of the N-atom acceptor was shown to have a strong effect on the reactivity: when a tertiary N-atom is involved in the 4-center elimination, the computed energy barrier is the lowest in all cases. The proposed rate rules were applied to 4 urea derivatives used in industry and they were able to establish the products branching ratios in the thermal decomposition of a given urea derivatives and to predict and compare their reactivity. Further work on the combustion kinetics of substituted isocyanates is needed to be able to develop combustion kinetic model for urea derivatives.

## Supporting Information

Isodesmic reactions, benchmark of computed lowest vibrational frequencies, high-pressure limit rate constants of two steps deamination, NASA polynomials of urea derivatives, bond dissociation energies of urea and carbamimidic acid, and PES of urea, N-methyl- and N,N-dimethyl-N'phenylurea.

## Acknowledgments

This project has received funding from the region Grand-Est (project CATCH). High performance computing resources were provided by IDRIS under the allocation A0100812434 made by GENCI and also by the EXPLOR center hosted by the University of Lorraine.

## References

(1) Wöhler, F. Ueber Künstliche Bildung Des Harnstoffs. *Ann. Phys.* **1828**, *88*, 253-256.

- (2) Skorupka, M.; Nosalewicz, A. Ammonia Volatilization from Fertilizer Urea—a New Challenge for Agriculture and Industry in View of Growing Global Demand for Food and Energy Crops. *Agriculture* **2021**, *11*, 822.
- (3) Kabo, G. Y.; Miroshnichenko, E. A.; Frenkel, M. L.; Kozyro, A. A.; Simirskii, V. V.; Krasulin, A. P.; Vorob'eva, V. P.; Lebedev, Y. A. Thermochemistry of Alkyl Derivatives of Urea. *Bull. Acad. Sci. USSR, Div. Chem. Sci.* **1990**, *39*, 662-667.
- (4) Kozyro, A. A.; Kabo, G. J.; Krasulin, A. P.; Sevruk, V. M.; Simirsky, V. V.; Sheiman, M. S.; Frenkel, M. L. Thermodynamic Properties of Methylurea. *J. Chem. Thermodyn.* **1993**, *25*, 1409-1417.
- (5) Emel'yanenko, V. N.; Kabo, G. J.; Verevkin, S. P. Measurement and Prediction of Thermochemical Properties: Improved Increments for the Estimation of Enthalpies of Sublimation and Standard Enthalpies of Formation of Alkyl Derivatives of Urea. *J. Chem. Eng. Data* **2006**, *51*, 79-87.
- (6) Dorofeeva, O. V.; Suchkova, T. A. Experimental Enthalpies of Formation and Sublimation of Urea Compounds: An Accuracy Assessment. *J. Chem. Thermodyn.* **2019**, *131*, 254-261.
- (7) Bodi, A.; Hemberger, P.; Gerber, T. A Robust Link between the Thermochemistry of Urea and Isocyanic Acid by Dissociative Photoionization. *J. Chem. Thermodyn.* **2013**, *58*, 292-299.
- (8) Gratzfeld, D.; Olzmann, M. Gas-Phase Standard Enthalpies of Formation of Urea-Derived Compounds: A Quantum-Chemical Study. *Chem. Phys. Lett.* **2017**, *679*, 219-224.
- (9) Chen, J. P.; Isa, K. Thermal Decomposition of Urea and Urea Derivatives by Simultaneous Tg/(Dta)/Ms. *J. Mass Spectrom. Soc. Jpn.* **1998**, *46*, 299-303.
- (10) Gratzfeld, D.; Heitkämper, J.; Debailleul, J.; Olzmann, M. On the Influence of Water on Urea Condensation Reactions: A Theoretical Study. *Z. Phys. Chem.* **2020**, *234*, 1311-1327.
- (11) Stein, M.; Bykov, V.; Bertótiné Abai, A.; Janzer, C.; Maas, U.; Deutschmann, O.; Olzmann, M. A Reduced Model for the Evaporation and Decomposition of Urea–Water Solution Droplets. *Int. J. Heat Fluid Flow* **2018**, *70*, 216-225.
- (12) Schaber, P. M.; Colson, J.; Higgins, S.; Thielen, D.; Anspach, B.; Brauer, J. Thermal Decomposition (Pyrolysis) of Urea in an Open Reaction Vessel. *Thermochim. Acta* **2004**, *424*, 131-142.
- (13) Brack, W.; Heine, B.; Birkhold, F.; Kruse, M.; Schoch, G.; Tischer, S.; Deutschmann, O. Kinetic Modeling of Urea Decomposition Based on Systematic Thermogravimetric Analyses of Urea and Its Most Important by-Products. *Chem. Eng. Sci.* **2014**, *106*, 1-8.
- (14) Krum, K.; Patil, R.; Christensen, H.; Hashemi, H.; Wang, Z.; Li, S.; Glarborg, P.; Wu, H. Kinetic Modeling of Urea Decomposition and Byproduct Formation. *Chem. Eng. Sci.* **2021**, *230*, 116138.
- (15) Tischer, S.; Börnhorst, M.; Amsler, J.; Schoch, G.; Deutschmann, O. Thermodynamics and Reaction Mechanism of Urea Decomposition. *Phys. Chem. Chem. Phys.* **2019**, *21*, 16785-16797.
- (16) Kuntz, C.; Kuhn, C.; Weickenmeier, H.; Tischer, S.; Börnhorst, M.; Deutschmann, O. Kinetic Modeling and Simulation of High-Temperature by-Product Formation from Urea Decomposition. *Chem. Eng. Sci.* **2021**, *246*, 116876.
- (17) Honorien, J.; Fournet, R.; Glaude, P. A.; Sirjean, B. Theoretical Study of the Gas-Phase Thermal Decomposition of Urea. *Proc. Combust. Inst.* **2021**, *38*, 355-364.
- (18) Tsepis, C. A.; Karipidis, P. A. Mechanistic Insights into the Bazarov Synthesis of Urea from  $\text{NH}_3$  and  $\text{CO}_2$  Using Electronic Structure Calculation Methods. *J. Phys. Chem. A* **2005**, *109*, 8560-8567.
- (19) Tokmakov, I. V.; Alavi, S.; Thompson, D. L. Urea and Urea Nitrate Decomposition Pathways: A Quantum Chemistry Study. *J. Phys. Chem. A* **2006**, *110*, 2759-2770.
- (20) Frisch, M. J.; Trucks, G. W.; Schlegel, H. B.; Scuseria, G. E.; Robb, M. A.; Cheeseman, J. R.; Scalmani, G.; Barone, V.; Petersson, G. A.; Nakatsuji, H.; et al. *Gaussian 16*; Revision C.01; Gaussian, Inc.: Wallingford, CT, 2016.
- (21) Montgomery, J. A.; Frisch, M. J.; Ochterski, J. W.; Petersson, G. A. A Complete Basis Set Model Chemistry. VI. Use of Density Functional Geometries and Frequencies. *J. Chem. Phys.* **1999**, *110*, 2822-2827.
- (22) Curtiss, L. A.; Redfern, P. C.; Raghavachari, K. Gaussian-4 Theory. *J. Chem. Phys.* **2007**, *126*, 084108.

- (23) Barnes, E. C.; Petersson, G. A.; Montgomery Jr, J. A.; Frisch, M. J.; Martin, J. M. Unrestricted Coupled Cluster and Brueckner Doubles Variations of W1 Theory. *J. Chem. Theory Comput.* **2009**, *5*, 2687-2693.
- (24) Zhao, Y.; Truhlar, D. G. The M06 Suite of Density Functionals for Main Group Thermochemistry, Thermochemical Kinetics, Noncovalent Interactions, Excited States, and Transition Elements: Two New Functionals and Systematic Testing of Four M06-Class Functionals and 12 Other Functionals. *Theor. Chem. Acc.* **2008**, *120*, 215-241.
- (25) Martin, J. M. L. Ab Initio Total Atomization Energies of Small Molecules — Towards the Basis Set Limit. *Chem. Phys. Lett.* **1996**, *259*, 669-678.
- (26) Woon, D. E.; Dunning Jr., T. H. Gaussian Basis Sets for Use in Correlated Molecular Calculations. V. Core-Valence Basis Sets for Boron through Neon. *J. Chem. Phys.* **1995**, *103*, 4572-4585.
- (27) Ruscic, B.; Pinzon, R. E.; Von Laszewski, G.; Kodeboyina, D.; Burcat, A.; Leahy, D.; Montoy, D.; Wagner, A. F. Active Thermochemical Tables: Thermochemistry for the 21st Century. In *Journal of Physics: Conference Series*, 2005; IOP Publishing: Vol. 16, p 078.
- (28) Ruscic, B.; Bross, D. H. *Active Thermochemical Tables (Atct) Values Based on Ver. 1.122r of the Thermochemical Network; Available at Atct.Anl.Gov.* 2021. (accessed 2022 08/24).
- (29) Bordwell, F. G.; Ji, G. Z. Effects of Structural Changes on Acidities and Homolytic Bond Dissociation Energies of the Hydrogen-Nitrogen Bonds in Amidines, Carboxamides, and Thiocarboxamides. *J. Am. Chem. Soc.* **1991**, *113*, 8398-8401.
- (30) Stradella, L.; Argentero, M. A Dsc, Tg, Ir Study of the Thermal Decomposition of Some Alkyl- and Aryl-Ureas. *Thermochim. Acta* **1995**, *268*, 1-7.
- (31) Vansteenkiste, P.; Van Neck, D.; Van Speybroeck, V.; Waroquier, M. An Extended Hindered-Rotor Model with Incorporation of Coriolis and Vibrational-Rotational Coupling for Calculating Partition Functions and Derived Quantities. *J. Chem. Phys.* **2006**, *124*, 044314.
- (32) Bryantsev, V. S.; Firman, T. K.; Hay, B. P. Conformational Analysis and Rotational Barriers of Alkyl- and Phenyl-Substituted Urea Derivatives. *J. Phys. Chem. A* **2005**, *109*, 832-842.
- (33) Dobrowolski, J. C.; Kofos, R.; Sadlej, J.; Mazurek, A. P. Theoretical and Ir-Matrix Isolation Studies on the Urea and Urea-D4, -13c, and -1,3-15n2 Substituted Molecules. *Vib. Spectrosc.* **2002**, *29*, 261-282.
- (34) Inostroza, N.; Senent, M. L. Large Amplitude Vibrations of Urea in Gas Phase. *Chem. Phys. Lett.* **2012**, *524*, 25-31.
- (35) Lizardo-Huerta, J. C.; Sirjean, B.; Bounaceur, R.; Fournet, R. Intramolecular Effects on the Kinetics of Unimolecular Reactions of B-Horo<sup>o</sup> and Hoq<sup>o</sup>Ooh Radicals. *Phys. Chem. Chem. Phys.* **2016**, *18*, 12231-12251, 10.1039/C6CP00111D.
- (36) Georgievskii, Y.; Klippenstein, S. *Mess. 2016.3.23*; Argonne National Laboratory, 2016.
- (37) Georgievskii, Y.; Miller, J. A.; Burke, M. P.; Klippenstein, S. J. Reformulation and Solution of the Master Equation for Multiple-Well Chemical Reactions. *J. Phys. Chem. A* **2013**, *117*, 12146-12154.
- (38) Tee, L. S.; Gotoh, S.; Stewart, W. E. Molecular Parameters for Normal Fluids. Lennard-Jones 12-6 Potential. *Ind. Eng. Chem. Fundam.* **1966**, *5*, 356-363.
- (39) Rowley, R.; Wilding, W.; Oscarson, J.; Yang, Y.; Giles, N. Dippr 801 Property Database, Software Package. *New York: Design Institute for Physical Property Data, American Institute of Chemical Engineers* **2009**.
- (40) Nicolle, A.; Cagnina, S.; de Bruin, T. First-Principle Based Modeling of Urea Decomposition Kinetics in Aqueous Solutions. *Chem. Phys. Lett.* **2016**, *664*, 149-153.
- (41) Luo, Y.-R. *Handbook of Bond Dissociation Energies in Organic Compounds*; 2002.
- (42) Manidhar, D.; Uma Maheswara Rao, K.; Suresh Reddy, C.; Syamasunder, C.; Adeppa, K.; Misra, K. An Improved Method for the Preparation of Alkyl/Arylurea Derivatives Using Chlorocarbonylsulfonyl Chloride as Carbonylating Agent. *Res. Chem. Intermed.* **2012**, *38*, 2479-2489.
- (43) Gupta, P. K. Chapter 24 - Herbicides and Fungicides. In *Biomarkers in Toxicology*, Gupta, R. C. Ed.; Academic Press, 2014; pp 409-431.
- (44) Chen, K.; Mackie, J. C.; Kennedy, E. M.; Dlugogorski, B. Z. Determination of Toxic Products Released in Combustion of Pesticides. *Prog. Energy Combust. Sci.* **2012**, *38*, 400-418.



- (45) Lizardo-Huerta, J. C.; Sirjean, B.; Verdier, L.; Fournet, R.; Glaude, P. A. The Decisive Role of Pericyclic Reactions in the Thermal Decomposition of Organophosphorus Compounds. *Proc. Combust. Inst.* **2021**, *38*, 719-727.
- (46) Lizardo-Huerta, J.-C.; Sirjean, B.; Verdier, L.; Fournet, R.; Glaude, P.-A. Thermal Decomposition of Phosgene and Diphosgene. *The Journal of Physical Chemistry A* **2018**, *122*, 249-257.
- (47) Song, Y.; Hashemi, H.; Christensen, J. M.; Zou, C.; Marshall, P.; Glarborg, P. Ammonia Oxidation at High Pressure and Intermediate Temperatures. *Fuel* **2016**, *181*, 358-365.
- (48) Glarborg, P.; Andreasen, C. S.; Hashemi, H.; Qian, R.; Marshall, P. Oxidation of Methylamine. *Int. J. Chem. Kinet.* **2020**, *52*, 893-906.
- (49) Pappijn, C. A.; Vermeire, F. H.; Van de Vijver, R.; Reyniers, M.-F.; Marin, G. B.; Van Geem, K. M. Combustion of Ethylamine, Dimethylamine and Diethylamine: Theoretical and Kinetic Modeling Study. *Proc. Combust. Inst.* **2021**, *38*, 585-592.
- (50) Altarawneh, I. S.; Altarawneh, M.; Rawadieh, S. E.; Almatarneh, M. H.; Shiroudi, A.; El-Nahas, A. M. Updated Yields of Nitrogenated Species in Flames of Ammonia/Benzene Via Introducing an Aniline Sub-Mechanism. *Combust. Flame* **2021**, *228*, 433-442.
- (51) Lizardo-Huerta, J.-C.; Sirjean, B.; Verdier, L.; Fournet, R.; Glaude, P.-A. Kinetic Modeling of the Thermal Destruction of Nitrogen Mustard Gas. *The Journal of Physical Chemistry A* **2017**, *121*, 3254-3262.
- (52) Glarborg, P.; Miller, J. A.; Ruscic, B.; Klippenstein, S. J. Modeling Nitrogen Chemistry in Combustion. *Prog. Energy Combust. Sci.* **2018**, *67*, 31-68.

## TOC Graphic

